Solar Energy Materials & Solar Cells ▮ (▮▮▮▮) ▮▮▮–▮▮▮

Contents lists available at SciVerse ScienceDirect

Solar Energy Materials & Solar Cells

journal homepage: www.elsevier.com/locate/solmat

Theoretical short-circuit current density for different geometries and organizations of silicon nanowires in solar cells

Martin Foldyna*, Linwei Yu, Pere Roca i Cabarrocas

Laboratory of Physics of Interfaces and Thin Films, LPICM, CNRS, Ecole Polytechnique, 91128 Palaiseau, France

ARTICLE INFO

Keywords:
Silicon nanowires
Solar cells
Optical modeling
Light trapping
Short circuit current density
Structure optimization

ABSTRACT

Radial junction solar cells are providing promising advantages of efficient light trapping and high built-in field when compared to their thin films or wafer based counter parts. In this work, we model short-circuit current densities for a wide range of nanowire arrays in order to define their optimal configurations. The modeling focuses on the fundamental nanowire properties, such as the nanowire length and the diameter, but also on their organization and on their density. The short-circuit current density is evaluated using rigorous coupled-waves analysis and normalizing the spectral absorptance by the standard AM 1.5 G solar spectrum. Results show that the nanowire density and length have the major impact on the device performance, while the nanowire organization is less important. Efficient light trapping properties of individual nanowires play an important role in the device performance and they have been further exploited in double-diameter nanowire arrays. An introduction of two different nanowire diameters into the same structure allowed for a separated optimization in two different spectral regions. As a result, we are reporting 10% increase in the short-circuit current density when double-diameter nanowire arrays were used.

1. Introduction

Recent boom in the solar cell industry has been caused primarily by the sufficient maturity of existing technologies and financial support of government entities promoting the renewable energy. In order to keep up with the growing energy consumption and to close the gap between prices of solar and fossil or nuclear energy, more innovations and technological advances are needed. Today's largest research efforts in the photovoltaic field are oriented towards maximizing the energy conversion efficiency while avoiding the inappropriate increase of the cost and thus reducing the price of the solar energy per kilowatt hour.

Thin film technologies provide an interesting alternative to the dominant silicon wafer based solar cells as they lead to more economical use of the silicon materials [1]. The major achievements for the amorphous silicon solar cells are represented by 10.1% overall efficiency [2], while tandem cells allows for as high as 11.9% efficiency [2]. Reported energy conversion efficiencies for triple junction thin film solar cells can be as high as 16.3% [3]. Further increase of the efficiency of a thin film based solar cell can be achieved by structuring the active region.

Very promising nanostructures for solar cells are silicon nanowires for their structural properties and possibility to make them in a crystalline silicon form. Nanowire based devices have high light trapping efficiency either due to efficient absorption of confined modes propagating through the vertical nanowires [4] or due to an enhanced scattering in the pseudo-random nanowire forests [5]. Both concepts represent material efficient solutions for enhanced light trapping required for a high performance photovoltaic device.

An economically viable approach for the nanostructured solar cells is the fabrication of silicon nanowires, either ordered in arrays or completely disordered. There are different methods to manufacture nanowires, e.g. by chemical etching into the crystalline silicon substrate [6] or vapor liquid solid method on different substrates including zinc oxide on glass or crystalline silicon [7–9]. Some of them allow for a more economical production (randomly oriented nanowires), while others can potentially overcome Yablonovitch limit [10] (vertically oriented nanowires).

The efficient light trapping inside nanowires has a very important application in the radial junction photovoltaic devices. Radial junction solar cells combine two important innovations to traditional solar cell designs: First, the active material itself is nanostructured and, second, the electrical field between p- and n-doped silicon is much stronger due to reduced distance between them. As a result, radial junction solar cells are not limited by the reduced carrier diffusion length, which is a typical problem for non-crystalline forms of silicon, e.g. amorphous phase silicon

* Corresponding author. Tel.: +33 169334311; fax: +33 169334333.
E-mail address: martin.foldyna@polytechnique.edu (M. Foldyna).

0927-0248/$ - see front matter © 2012 Elsevier B.V. All rights reserved.
http://dx.doi.org/10.1016/j.solmat.2012.10.014

(thickness limited to 300 nm) or micro-crystalline silicon (often limited to 2 μm). The thickness of the intrinsic layer in p-i-n or n-i-p radial junction can be rather small (less than 100 nm [11,7]), while still allowing for a long nanowire length and excellent light trapping properties. This innovative approach opens the door for a new generation of solar cells with a nanostructured active layer as well as engineered build-in electromagnetic field intensity [12]. As it will be shown in Section 3, the efficient light trapping behavior of vertical nanowires is based mainly on the propagation of the light in the form of confined modes inside individual nanowires. This has an important implication of a relatively high tolerance of the manufacturing processes to the geometrical dimensions and nanowire organizations which is beneficial for the fabrication of nanowire based devices. Finally, this tolerance opens possibilities for less perfect (in the sense of periodicity), but also less expensive, fabrication of the nanowire based solar cells.

In the next section we introduce theoretical background for absorptance and short-circuit current calculations. Effects of structural parameters on light trapping effects inside vertical nanowire arrays are shown in Section 3, where the absorption inside vertical silicon nanowires under normal incidence is governed by an efficient light confinement. Theoretical short-circuit current calculated using AM 1.5 G spectrum is shown for different nanowires lengths, diameters and pitches. Dependence of the short-circuit current on the diameter and the pitch is shown for multiple nanowires lengths in the form of maps, for each nanowire organization separately. Maximal values of the short-circuit current are plotted as a function of the length showing nonlinear increase and comparable values between square and hexagonal nanowire arrays. Section 3 finishes with the introduction of a double-diameter nanowire structure allowing for further improvement of the device performance. The results are shortly concluded in Section 4.

2. Theory

In our work, vertical crystalline silicon nanowires are arranged into two-dimensional grids with supporting silver substrate as shown in Fig. 1. The incoming light is considered as a linearly polarized planar wave of a selected wavelength that approaches the structure at normal incidence. In the model, a silver substrate bellow nanowire arrays was used in order to avoid a situation where significant portion of the light is transmitted through the nanowire layer. A mirror or a highly reflective structure is always present at the bottom of the solar cell for increasing of the light absorption and current. The goal of the study will be to compare different configurations of nanowire diameters, densities, lengths and organizations and to show preferred combinations of these parameters for the optimal performance.

The optical response of silicon nanowires organized in a periodic arrays was modeled using 3D rigorous coupled-waves analysis (RCWA) [13,14]. The method is based on Fourier series expansions of a periodic electromagnetic field inside the structure with boundary conditions connecting tangential field components at interfaces between layers. The convergence of the method has been improved using inverse rules [15] and the scattering matrix approach for deeper structures (longer nanowires) [16].

The distribution of electromagnetic field was calculated in order to demonstrate efficient light trapping properties of silicon nanowire arrays. In this work we show either vertical cross-section through the middle of the nanowire or horizontal plane at the specified nanowire height. From the obtained electromagnetic field, the Poynting vector has been calculated as

$$\mathbf{P} = \Re(\mathbf{E} \times \mathbf{H}), \tag{1}$$

where **E** and **H** are vectors of the electric and the magnetic field, respectively. The symbol $\Re$ denotes the real part of a complex function or a number. For a clear illustration of energy losses during the wave propagation, the normal component of Poynting vector was calculated as follows:

$$P_z = \Re(E_x H_y - E_y H_x), \tag{2}$$

where E_x, E_y, H_x, and H_y denote the tangential components of the electric and magnetic field, respectively.

The RCWA does not provide the electromagnetic field distribution directly, as for instance finite-difference time-domain (FDTD) method [17] or finite elements method (FEM) [18] do, but the field can be reconstructed from the complete scattering matrix of the structure together with eigenvalues and eigenvectors inside each layer. The spatial distribution of the electromagnetic field is calculated as a sum of Fourier series expansion of all eigen modes,

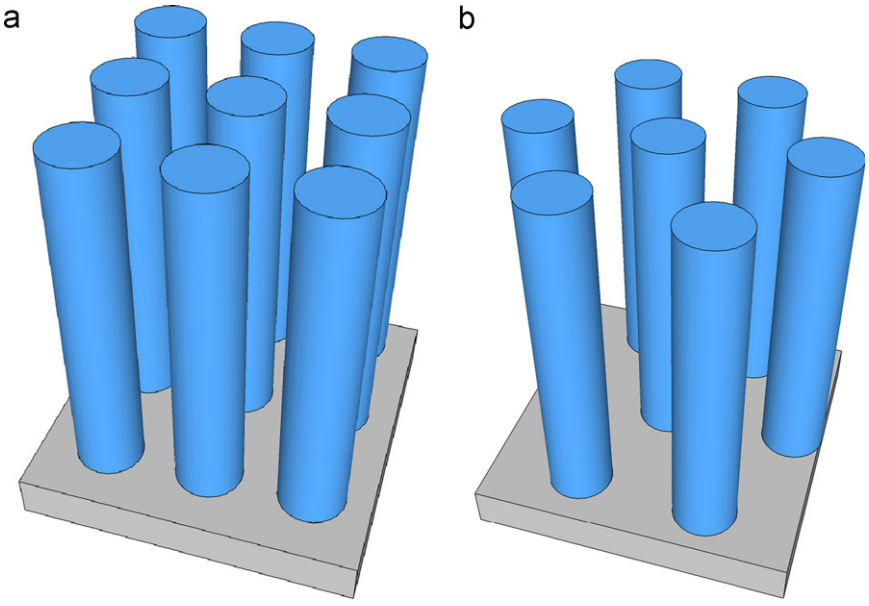

Fig. 1. Two different configurations of nanowire arrays on a silver mirror. Nanowires are organized either in (a) square periodic grid or (b) densely packed hexagonal periodic grid.

Please cite this article as: M. Foldyna, et al., Theoretical short-circuit current density for different geometries and organizations of silicon nanowires in solar cells, Solar Energy Materials and Solar Cells (2012), http://dx.doi.org/10.1016/j.solmat.2012.10.014

with appropriate amplitudes acquired by the RCWA, at each selected point. The reason why we have used the RCWA method instead of other methods is an advantage of faster calculation speed, which was very important for this work, as figures and data presented in this work represent millions of 3D calculations.

The amount of light absorbed in the nanowire array, calculated using the RCWA, does not give a direct information about the potential performance of the device. In order to better evaluate the performance of silicon nanowire based photovoltaic devices, the absorptance was transformed into the short-circuit current density (J_{sc}) using the standard solar spectrum (AM 1.5 G). The values calculated using the following formula can be used to estimate maximum J_{sc} under the condition that every absorbed photon (with energy larger than the bandgap) leads to a carrier separation followed by a successful carrier collection:

$$J_{sc} = e\int_E A(E)N(E)\,\mathrm{d}E. \tag{3}$$

Here $A(E)$ is the absorptance inside nanowires as a function of the incident photon energy E, $N(E)$ is the number of photons per unit area per second for the energy E from the standard solar spectrum, and e is the electron charge. Short-circuit current density from Eq. (3) provides an upper estimate of the short circuit current achievable for a given nanowire geometry. Note that the value of the theoretical maximum of J_{sc} for the crystalline silicon is around 46 mA/cm^2.

3. Results and discussions

The efficient light trapping of silicon nanowire arrays is based on individual effects of each single nanowire, which traps the light inside in the form of confined propagating modes. The confinement is very efficient in the case of matching resonance condition on the nanowire walls and can reach almost 100% in the blue part of the spectrum, where silicon has a very high absorption. Note that the absorption in the nanowire does not happen only for a selected diameter-wavelength resonance condition. The confinement of the light is still significant, although with a slightly reduced efficiency, in the case where the diameter is larger than required for the resonance condition. In such case there is some leakage of the electromagnetic field outside of the nanowire, but the major part of the energy still propagates through the nanowire core. In the case of a sufficiently large diameter (when compared to the wavelength) the light can be again efficiently confined inside of the nanowire in the form of the higher order resonant mode.

In Fig. 2 we plotted the spatial distribution of the normal component of Poynting vector (power flux) inside nanowires with diameters of 200 nm and lengths of 2 μm organized in periodic hexagonal arrays. Four subfigures in Fig. 2(a)–(d) show the situation for four different pitches of 0.4, 0.6, 0.8 and 1 μm, respectively. The strong confinement of the light inside the nanowires can be observed for all four selected pitches and it is clear that this effect is not depending on the pitch itself. In other words, the observed strong light confinement is a property of every single individual nanowire and it will be still present in the cases of disordered vertical nanowire arrays.

The spectral dependence of the calculated absorptance is shown in Fig. 3 including corresponding spatial distribution of the normal component of Poynting vector at selected wavelengths. The notable confinement of the energy flow inside nanowires is observable at almost any wavelength, which is permitted by relatively large 200 nm nanowire diameters. The nanowire diameter is not the only obvious parameter having strong impact on the light trapping efficiency. It is natural to expect that the absorptance increases significantly when the nanowire length is increased.

The spectral dependence of the absorptance for three different nanowire lengths is shown in Fig. 4. Selected spectra represent the highest values of J_{sc} acquired for square nanowire arrays at given nanowire lengths. The lengths of 1, 3 and 7.5 μm were selected in order to show that the absorption edge shifts towards the near infrared part of the spectrum with increasing nanowire lengths. Obviously, the longer nanowires the higher J_{sc} values can be achieved with a maximum for infinitely long nanowire arrays.

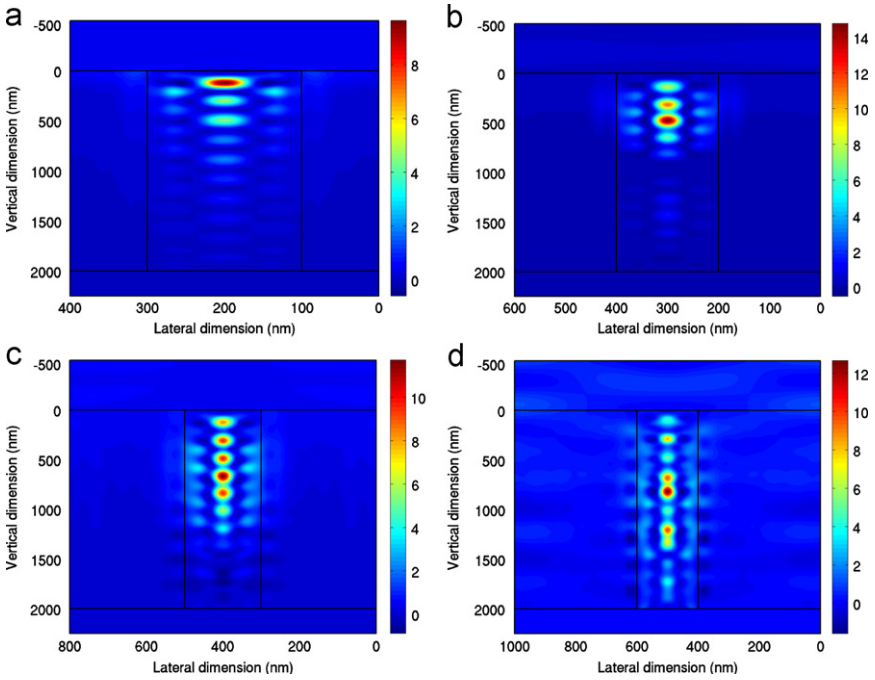

Fig. 2. Maps of normal component of Poynting vector shown for the same nanowires, but organized in hexagonal arrays of different pitches (0.4, 0.6, 0.8 and 1 μm). Vertical cross-section is plotted at wavelength of 500 nm, nanowire diameter of 200 nm and length of 2 μm. (a) 400 nm pitch; (b) 600 nm pitch; (c) 800 nm pitch; and (d) 1000 nm pitch.

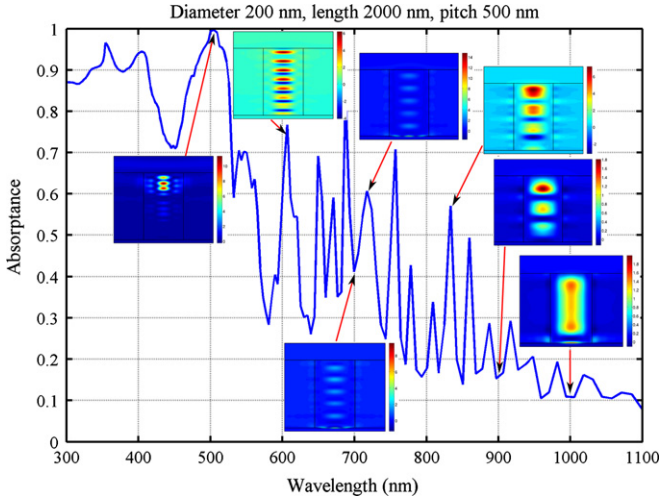

Fig. 3. Spectral dependence of absorptance together with spatial distributions of a normal component of the Poynting vector shown for selected wavelengths, similar to Fig. 2. Nanowires have 200 nm diameters, 2 μm length and are organized in square arrays of 500 nm pitch.

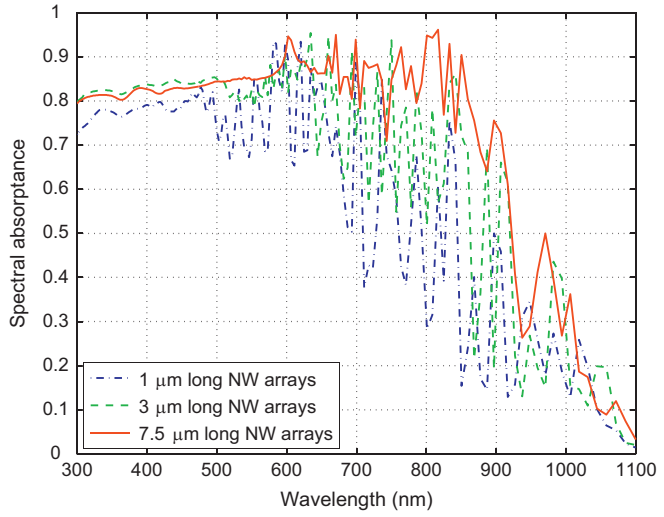

Fig. 4. Spectral dependence of absorptance for three different nanowire diameters of 420 nm and lengths of 1, 3 and 7.5 μm, respectively. Square nanowire array pitches are 580, 620 and 600 nm, respectively. The short circuit current densities (J_{sc}) are 24.7, 29.1 and 32.3 mA/cm^2, respectively.

Nevertheless, there are many technical difficulties with the fabrication of very long and dense nanowire arrays, such samples would be very fragile and it would be extremely difficult to coat them with a doped silicon layer and a transparent conducting oxide.

A rational optimization of silicon nanowire based solar cells requires systematic study and analysis of effects of nanowire density, diameters, lengths and organization in order to evaluate parameter sets leading to the high light trapping efficiency, but without sacrificing fabrication feasibility. We have started our analysis by mapping J_{sc} values for the whole range of nanowire diameters and pitches (from 100 nm to 700 nm) for both types of nanowire organizations as illustrated in Fig. 1. The evaluation has been performed for various nanowire lengths (from 1 μm to 10 μm) as this parameter is usually fixed by a fabrication process due to the linear dependence of the nanowire manufacturing time on the nanowire length.

Results of the analysis are shown in Fig. 5 for nanowire lengths of 3 μm and 5 μm and both types of arrays (square and hexagonal periodic grid arrays). Values of J_{sc} have a striking resemblance when compared between the square and the hexagonal periodic array. This is due to the previously mentioned fact that the strongest light trapping effect of nanowires is based on the individual wave-guiding like propagation of confined modes which does not require strictly periodic arrangement and therefore, the dependence on the nanowire organization is rather small. There are, however, some differences due to different definitions of pitch which leads to different densities for different nanowire array organizations. While the density in square arrays can be defined as $D_s = \pi r^2/\Lambda_s^2$, where r denotes the nanowire diameter and Λ_s is the pitch; the density in hexagonal arrays is defined as $D_h = 2\pi r^2/\sqrt{3}\Lambda_h^2$ with Λ_h denoting the distance between the closest nanowire centers. By relating them and assuming the same pitch ($\Lambda_s = \Lambda_h$) we get a ratio

$$\frac{D_h}{D_s} = \frac{2}{\sqrt{3}}, \tag{4}$$

between the density of nanowires organized in hexagonal arrays and the density of nanowires organized in square arrays, respectively. As a result, hexagonal arrays have around 15% higher material density than square arrays for the same value of pitch in Fig. 5. That is a reason why the highest J_{sc} values are somewhat shifted to the higher pitches for hexagonal organized nanowires. The maximum value of J_{sc} can be found around nanowire diameter of 420 nm and the pitch of 650 nm for 5 μm long nanowires in periodic square arrays, while for the hexagonal arrays the maximum value is found around the pitch of 700 nm. Note that the maximum J_{sc} value is found for similar nanowire densities for both studied nanowire array organizations, which means that the nanowire density is a key parameter for an optimal device performance.

Dependence of J_{sc} on the nanowire diameter and the pitch in Fig. 5 shows very similar values for large range of parameters. That supports the idea that nanowire arrays, as presented in this work, have high tolerance to manufacturing processes and that reasonably large change in the diameter, pitch or nanowire length will not lead to a dramatic drop in the device performance. Nevertheless, it is important to specify the best potential values of J_{sc} which can be obtained for the devices of similar geometries as shown in this paper. In order to evaluate the potential of nanowire based solar cells, we have determined the maximum value of J_{sc} for nanowire lengths between 1 μm and 10 μm. Results for both nanowire array organizations (in square and hexagonal arrays, see Fig. 1) are shown in Fig. 6. Maximum values are almost identical for both configurations up to the length of 5 μm with a logarithmic dependence on the nanowire length. The reason why square arrays have higher values for longer nanowires is that due to their different density dependencies on the pitch [see Eq. (4)], maximum values for hexagonal arrays are shifted towards larger pitches, potentially leaving our area of interest (diameter sizes from 100 nm to 700 nm and pitches from 200 nm to 700 nm). Practical limit for the nanowire length taken from Fig. 6 is around 5 μm due to the relatively steep growth of values paying off the longer fabrication time and the larger cost. After 5 μm, the logarithmic dependence of J_{sc} does not usually pay off the increased cost and decreased mechanical stability.

A significant and not yet discussed way to further boost the device performance is to introduce double-diameter nanowire arrays, which combines nanowires of two different diameters in the same array. Different nanowire diameters have maximum absorptance at different wavelengths as it was illustrated before. Therefore, it is important to choose an appropriate value for the full-range optimization of the device. If we imagine more than one diameter present in our structure, such geometry allows for the new level of optimization which can tune specific resonance modes to specific wavelengths, e.g. one for shorter wavelengths

Please cite this article as: M. Foldyna, et al., Theoretical short-circuit current density for different geometries and organizations of silicon nanowires in solar cells, Solar Energy Materials and Solar Cells (2012), http://dx.doi.org/10.1016/j.solmat.2012.10.014

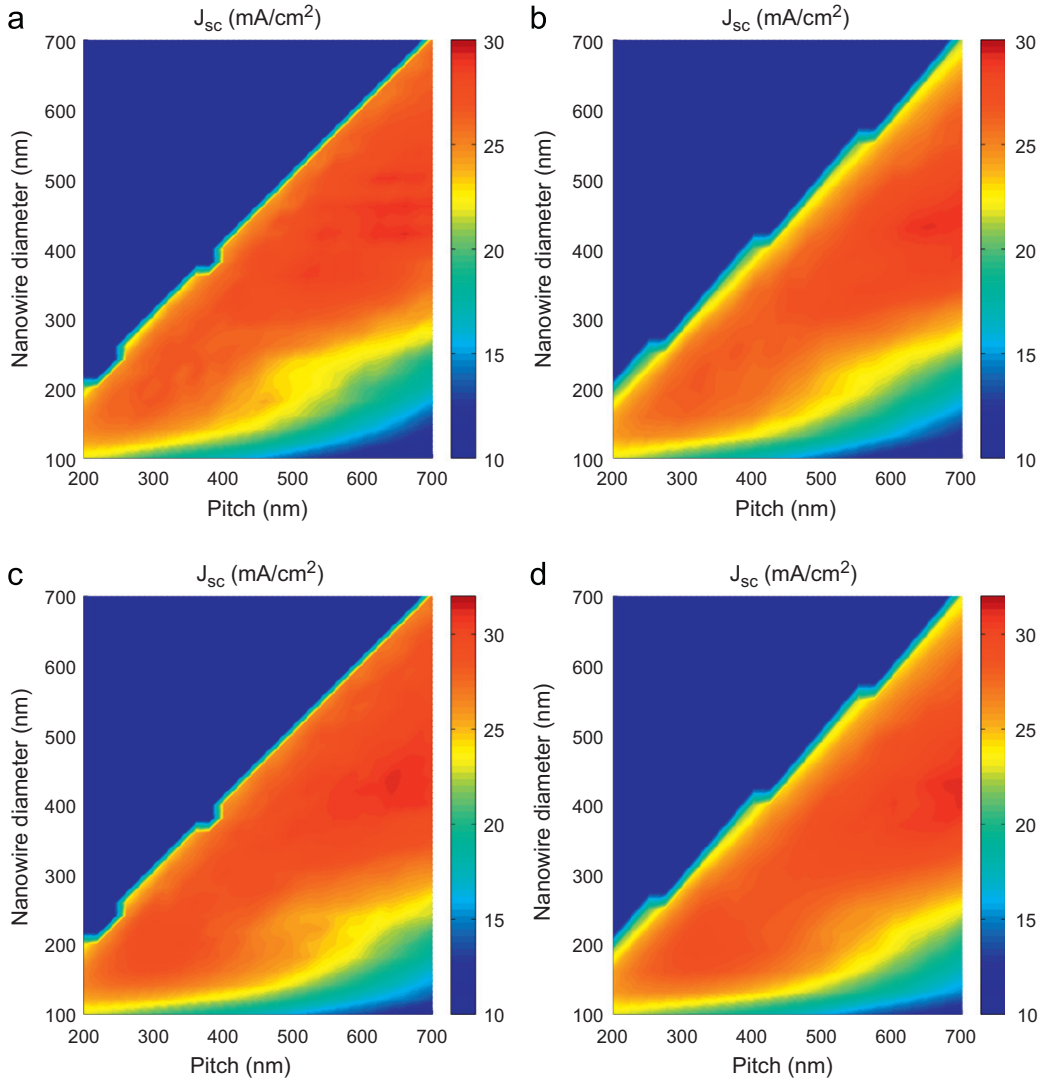

Fig. 5. Short-circuit current density as a function of the nanowire diameter and the pitch. Plots at the top correspond to nanowire lengths of 3 μm while bottom ones correspond to lengths of 5 μm. Left and right plots correspond to square and hexagonal nanowire arrays, respectively. (a) 3 μm long, square arrays; (b) 3 μm long, hexagonal arrays; (c) 5 μm long, square arrays; and (d) 5 μm long, hexagonal arrays.

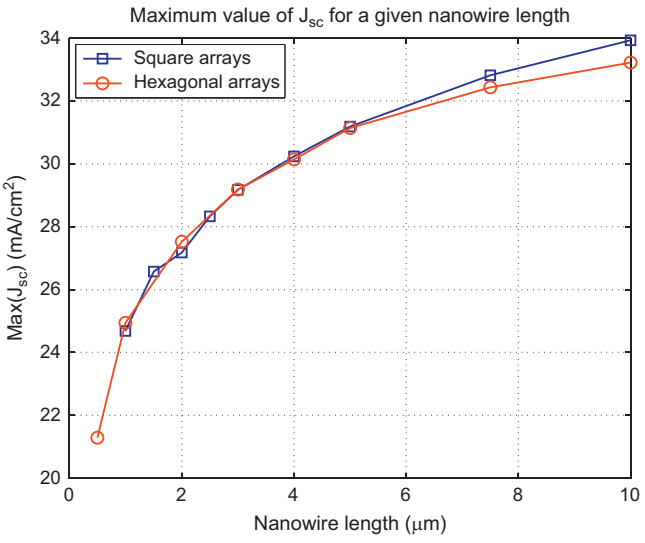

Fig. 6. Dependence of the largest J_{sc} value on the nanowire length for the square and hexagonal nanowire arrays, respectively. The maximum is evaluated for diameters and pitches below 700 nm.

and second one for longer ones. This structure is enabled by a large effective cross-section of the nanowire which is much larger than its physical cross-section . The idea is demonstrated in Fig. 7 on the spatial distribution of energy flow over the unit cell of the double-diameter structure. The left subfigure in Fig. 7 shows normal component of Poynting vector at wavelength of 450 nm, where nanowires of both diameters (the smaller is 100 nm and the larger is 200 nm) allow for the propagation of confined modes. In contrast, the right subfigure of Fig. 7 shows that at wavelength of 700 nm only the 200 nm diameter nanowire in the center effectively traps the light inside.

Following the previous demonstration, we have modeled J_{sc} for double-diameter structures at a fixed nanowire length of 3 μm and with the distance between the closest nanowires fixed at 600 nm. Resulting values for nanowire diameters between 0 and 600 nm are shown in Fig. 8. We can observe that the higher values are present when at least one of the diameters is larger than 300 nm. The detailed view in Fig. 9 reveals clear increase of J_{sc} values in asymmetric cases where diameters are not equal. Values of J_{sc} increased from around 27 mA/cm^2 to about 29.5 mA/cm^2, which corresponds to an increase close to 10%. This increase is substantial while still maintaining the relative structural simplicity.

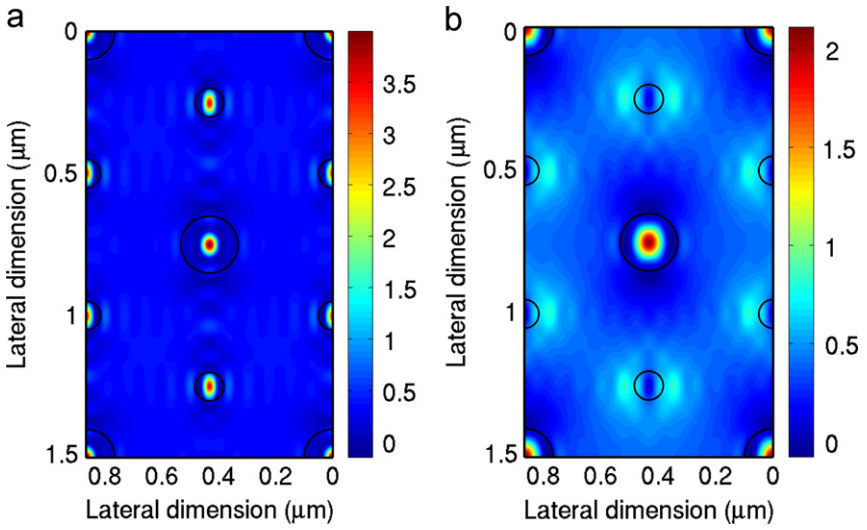

Fig. 7. Normal component of Poynting vector from Eq. (2) plotted at wavelength of 450 nm and 700 nm, respectively. Cross-section plane is positioned at $\lambda/3.5$ below the top of nanowires. Smaller nanowire diameters are 100 nm while larger ones correspond to 200 nm and the distance between closest neighbors is 500 nm. (a) Wavelength of 450 nm and (b) wavelength of 700 nm.

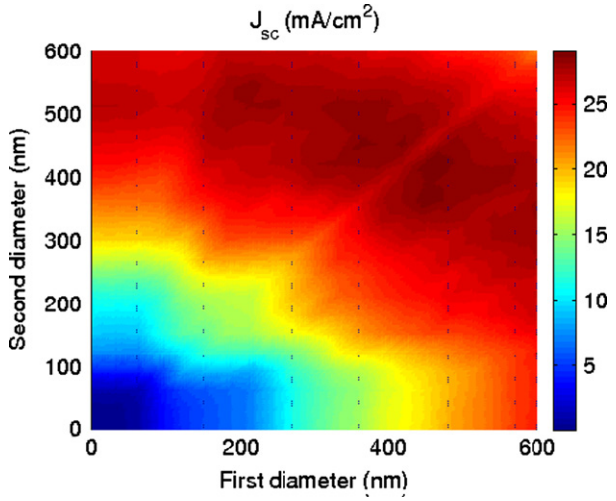

Fig. 8. Short circuit current density as a function of two silicon nanowire diameters. The pitch was fixed at 600 nm and the nanowire length at 3 μm for all cases.

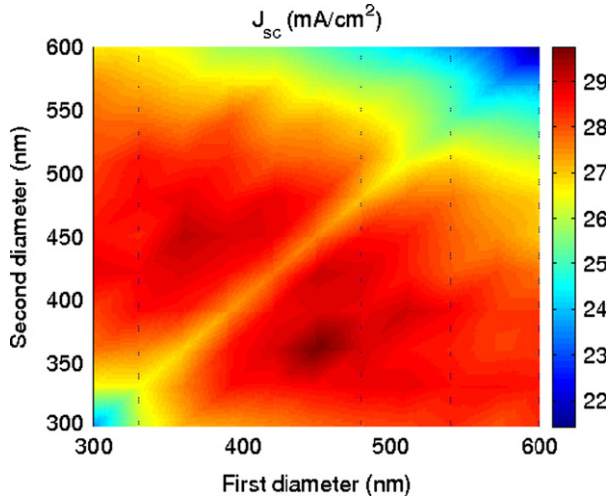

Fig. 9. Detailed view on J_{sc} under the same conditions as in Fig. 8 (color scale has been adjusted in this plot). (For interpretation of the references to color in this figure caption, the reader is referred to the web version of this article.)

Multi-dimensional calculations including the pitch, two diameters and the nanowire length are computationally very heavy, preventing the simple scanning through all four parameter dimensions unless quite substantial calculation time is devoted to it. The situation becomes even more complicated if the rest of structural parameters of the complete solar cell are considered, e.g. an active layer below silicon nanowires to further improve the absorptance and J_{sc}, the thickness of the top transparent conducting oxide electrode, the diameter of the doped silicon nanowire core, etc. Clearly, an efficient and optimized design requires some simplifications in the form of empirical rules which bring more clarity and allow for considerable savings of the calculation time.

4. Conclusions

In this work, we have presented a systematic modeling of the impact of critical parameters defining nanowire arrays, i.e. the nanowire diameter and length, the pitch and the organization of arrays, on the solar cell performance. We have shown that the J_{sc} values are not very dependent on the array organization (square versus hexagonal grids) and that parameters with the strongest impact on J_{sc} values are the nanowire length and density. The idea of using double-diameter nanowire arrays has been introduced and we have shown the potential of 10% gain on J_{sc} values by combining proper diameter sizes. We have contributed to better clarity and the intuitive understanding of the optical absorption inside nanowire arrays, their (in)dependence on the organization and the new double-diameter design.

Acknowledgment

This work has been performed in the framework of the Total-LPICM-CNRS Joint PV research team.

References

[1] M. Konagai, Present status and future prospects of silicon thin-film solar cells, Japanese Journal of Applied Physics 50 (2011) 030001–1–12.
[2] M. Green, Solar cell efficiency tables (version 37), Progress in Photovoltaics: Research and Applications 19 (2011) 84–92.

Please cite this article as: M. Foldyna, et al., Theoretical short-circuit current density for different geometries and organizations of silicon nanowires in solar cells, Solar Energy Materials and Solar Cells (2012), http://dx.doi.org/10.1016/j.solmat.2012.10.014

[3] B. Yan, G. Yue, L. Sivec, J. Yang, S. Guha, C.-S. Jiang, Innovative dual function nc-siox:h layer leading to a $>16\%$ efficient multi-junction thin-film silicon solar cell, Applied Physics Letters 99 (2011) 113512.
[4] J. Wang, Z. Li, N. Singh, S. Lee, Highly-ordered vertical Si nanowire/nanowall decorated solar cells, Optics Express 19 (2011) 23078–23084.
[5] L. Yu, F. Fortuna, B. O'Donnell, T. Jeon, M. Foldyna, G. Picardi, P. Roca i Cabarrocas, Bismuth-catalyzed and doped silicon nanowires for one-pump-down fabrication of radial junction solar cells, Nano Letters 12 (2012) 4153–4158.
[6] E. Garnett, P. Yang, Light trapping in silicon nanowire solar cells, Nanoletters 10 (2010) 1082–1087.
[7] L. Yu, B. O'Donnell, M. Foldyna, P. Roca i Cabarrocas, Radial junction amorphous silicon solar cells on PECVD-grown silicon nanowires, Nanotechnology 23 (19) (2012) 194011.
[8] T. Stelzner, M. Pietsch, G. Andra, F. Falk, E. Ose, S. Christiansen, Silicon nanowire-based solar cells, Nanotechnology 19 (2008) 295203.
[9] M. Kelzenberg, S. Boettcher, J. Petykiewicz, D. Turner-Evans, M. Putnam, E. Warren, J. Spurgeon, R. Briggs, N. Lewis, H. Atwatter, Enhanced absorption and carrier collection in si wire arrays for photovoltaic applications, Nature Materials 9 (2010) 239–244.
[10] D.F. Sievenpiper, E. Yablonovitch, J.N. Winn, S. Fan, P.R. Villeneuve, J.D. Joannopoulos, 3D metallodielectric photonic crystals with strong capacitive coupling between metallic islands, Physical Review Letters 80 (1998) 2829.
[11] L. Yu, B. O'Donnell, P.-J. Alet, S. Conesa-Boj, F. Peiro, J. Arbiol, P. Roca i Cabarrocas, Plasma-enhanced low temperature growth of silicon nanowires and hierarchical structures by using tin and indium catalysts, Nanotechnology 20 (22) (2009) 225604.
[12] J. Zhu, Z. Yu, S. Fan, Y. Cui, Nanostructured photon management for high performance solar cells, Materials Science and Engineering: R 70 (2010) 330–340.
[13] M.G. Moharam, T.K. Gaylord, Diffraction analysis of dielectric surface-relief gratings, The Journal of the Optical Society of America 72 (10) (1982) 1385–1392.
[14] L. Li, Fourier modal method for crossed anisotropic gratings with arbitrary permittivity and permeability tensors, Journal of Optics A: Pure and Applied Optics 5 (2003) 345–355.
[15] L. Li, Use of fourier series in the analysis of discontinuous periodic structures, The Journal of the Optical Society of America A 13 (9) (1996) 1870–1876.
[16] L. Li, Formulation and comparison of two recursive matrix algorithms for modeling layered diffraction gratings, The Journal of the Optical Society of America A 13 (1996) 1024–1035.
[17] K. Yee, Numerical solution of initial boundary value problems involving maxwell's equations in isotropic media, IEEE Transactions on Antennas and Propagation 14 (3) (1966) 302–307.
[18] A. Hrennikoff, Solution of problems of elasticity by the frame-work method, Journal of Applied Mechanics, Transactions ASME 8 (1941) A169–A715.

Please cite this article as: M. Foldyna, et al., Theoretical short-circuit current density for different geometries and organizations of silicon nanowires in solar cells, Solar Energy Materials and Solar Cells (2012), http://dx.doi.org/10.1016/j.solmat.2012.10.014